ELSEVIER

Journal of Molecular Liquids 136 (2007) 221 – 226

journal of MOLECULAR LIQUIDS

www.elsevier.com/locate/molliq

Understanding how organic solvent polarity affects water structure and bonding at halocarbon–water interfaces

Cathryn L. McFearin, Geraldine L. Richmond *

Department of Chemistry and Materials Science Institute, University of Oregon, Eugene, OR 97403, United States

Available online 24 August 2007

Abstract

Vibrational sum-frequency spectroscopy (VSFS) is employed here to study the bonding and structure of water molecules at the mixed halocarbon–water interface. Mixtures of non-polar CCl_4 with more polar solvents $CHCl_3$, dichloromethane (DCM), and 1,2-dichloroethane (DCE) are used to vary the polarity of the organic phase. The OH stretching modes of interfacial water molecules are used to characterize and compare the interactions between water and the different halocarbons in the organic phase. The spectroscopic results show differing degrees of interaction between water and the various halocarbon molecules in the interfacial region as manifested in spectral shifts and intensity changes in the OH stretching modes. The spectral observations indicate that as the organic phase is systematically increased in polarity with the addition of polar halocarbons, the interfacial water molecules display increased bonding interactions with the organic phase. This increased interaction between interfacial water and the interfacial halocarbons leads to a reduction in the strong orientation of interfacial water molecules that is so prevalent for water adjacent to non-polar organic liquids. The results provide important insights into water adjacent to a hydrophobic surface as that surface takes on increasingly polar characteristics.
Published by Elsevier B.V.

Keywords: Liquid–liquid interfaces; Water at hydrophobic surfaces; Hydrogen bonding; Vibrational sum-frequency spectroscopy

1. Introduction

1.1. The liquid–liquid interface

There has been a growing interest in recent years in the molecular structure of the liquid–liquid interface due in part to its applicability and relevance to a variety of scientific disciplines [1]. It has long been of interest to electrochemists because of the ability to polarize selected liquid–liquid interfaces and induce ion and electron transport. For biochemists, the liquid–liquid interface is a model for understanding molecular assembly and ion transport. Other important applications include solvent extraction, phase-transfer catalysis, and nanoparticle formation. Because these and other important interfacial events are reliant on the characteristics of the liquid–liquid interface, detailed knowledge of the chemical and structural nature of the interface is necessary to advance the understanding and development of these diverse branches of scientific research.

Many different studies have been conducted in attempts to answer the central questions regarding the structure and interactions present at liquid–liquid interfaces. Some of the important work in this area includes X-ray studies done by Schlossman and coworkers that determine structural properties such as the interfacial widths of different liquids at the interface with water [2–6]. Second harmonic generation (SHG) is a surface specific spectroscopic technique that has been used to explore the effects of surface charge on solvation by Walker et al. [7]. Recently Eisenthal and coworkers have also used SHG to look at ultrafast electron transfer at the liquid–liquid interface [8]. The field has also benefited from theoretical studies. Molecular dynamics (MD) and Monte Carlo simulations done on liquid–liquid systems have contributed greatly towards the understanding of the microscopic interactions at the interface [9–21].

In recent years another surface specific technique that has been demonstrated to provide molecular level information about interfaces is vibrational sum-frequency spectroscopy (VSFS). Previous liquid–liquid studies done in the Richmond laboratory using VSFS have shown that non-polar liquids, CCl_4 and the C_6–C_8 *n*-alkanes, in contact with water form relatively sharp

* Corresponding author. Tel.: +1 541 346 4635; fax: +1 541 346 5859.
E-mail address: richmond@uoregon.edu (G.L. Richmond).

0167-7322/$ - see front matter. Published by Elsevier B.V.
doi:10.1016/j.molliq.2007.08.004

interfaces with weak interactions between the two phases that lead to interfacial water with a high degree of orientation [22–24]. The next step towards understanding the structure and interactions at liquid interfaces is to use VSFS to look at a more polar liquid in contact with water to see what effect stronger water–organic interactions have on interfacial properties. Earlier VSFS studies of the 1,2-dichloroethane (DCE)/water interface have suggested that increased interactions between the more polar DCE and water lead to a more diffuse and a less ordered interface [25].

The studies presented here use VSFS to obtain a more detailed picture of the effect of the variation of the polarity of the organic liquid on the structure and bonding of the interfacial water molecules. This paper builds on the previous work by Walker et al, described above, with more detailed work on the effect of the addition of polar organic solvents to the non-polar CCl_4 organic phase [25]. By using mixtures of three polar liquids ($CHCl_3$, dichloromethane (DCM), and 1,2-dichloroethane (DCE)) that have different dipole moments with non-polar CCl_4, the polarity of the organic phase is altered systematically to look at the effects on the interfacial structure. The dipole moment values for $CHCl_3$ and DCM are 1.04 D and 1.60 D respectively. DCE has a dipole moment of 2.1 D for the gauche conformation. Simulation results have shown that a higher population of that form exists at the interface than in bulk DCE [9]. Comparison of the vibrational spectra of interfacial water in these mixture studies with that obtained for CCl_4/water, allows us to monitor how the polarity of the organic phase affects the interfacial water structure and the interactions between water and halocarbon molecules that are present at the interface [23,24].

1.2. Background of VSFS

In VSFS two laser beams are overlapped at an interface, generating a third beam at the sum of the frequencies of the two incident beams. For the experiments presented here, one beam is at a fixed visible frequency and one is tunable over a range of infrared frequencies. An outline of the important aspects of VSFS is given here. More detailed treatments can be found in the literature [26–34]. The intensity $I(\omega_{SF})$ of the VSFS light generated at the interface is given by

$$I(\omega_{SF}) \propto |\chi^{(2)}|^2 I(\omega_{IR}) I(\omega_{VIS}) \tag{1}$$

where $I(\omega_{IR})$ and $I(\omega_{VIS})$ are the respective intensities of the incoming tunable infrared and visible beams and $\chi^{(2)}$ is the macroscopic second order non-linear susceptibility. $\chi^{(2)}$ is composed of a non-resonant term, $\chi^{(2)}_{NR}$, and a resonant susceptibility term, $\chi^{(2)}_{\upsilon}$. The resonant term can be written as

$$\chi^{(2)}_{\upsilon} \propto \frac{NA_{\upsilon}}{\omega_{\upsilon} - \omega_{IR} - i\Gamma_{\upsilon}} \tag{2}$$

where N is the number density of molecules, A_{υ} is the product of the Raman and IR transition moments, ω_{υ} is the vibrational transition frequency, ω_{IR} is the tunable IR frequency, and Γ_{υ} is the linewidth of the transition. Non-resonant contributions have not been detected in these liquid–liquid studies so $\chi^{(2)}_{NR}$ is observed to be zero. As the IR is tuned over a range of frequencies and ω_{IR} approaches a resonance ω_{υ} there is an increase in VSFS intensity producing a vibrational spectrum of interfacial molecules. These susceptibility terms are complex quantities that have both phases and amplitudes. Because the VSFS intensity is related to the square of the sum of these susceptibility terms, the resulting spectrum can have either constructive or destructive interferences between contributions from different interfacial modes.

The inherent surface specificity of VSFS lies in the term A_{υ}, which shows that a molecular vibration will be VSFS active only if it is both IR and Raman active. This result along with the coherent nature of VSFS excludes centrosymmetric media from contributing to VSFS signal. The non-centrosymmetric nature of an interface makes VSFS capable of distinguishing between the isotropic bulk media and surface molecules. In addition to the surface specificity of VSFS, orientation information about the molecules at the interface can be obtained by choosing polarizations of the beams that correspond to different components of the $\chi^{(2)}_{\upsilon}$ tensor. All spectra that are described below were taken in the SSP polarization scheme (SF=S, VIS=S, IR=P), which probes vibrational modes that have a component of their transition dipole perpendicular to the interfacial plane. The macroscopic term $\chi^{(2)}_{\upsilon}$ is related to the microscopic property, the molecular hyperpolarizability β_{υ}, by Eq. (3) via the number density of the interfacial molecules N and an orientationally averaged Euler angle transformation $\langle \mu_{IJK:lmn} \rangle$ from the molecular coordinates (l, m, n) to the laboratory coordinates (I, J, K).

$$\chi^{(2)}_{\upsilon} = N \sum_{lmn} \langle \mu_{IJK:lmn} \rangle \beta_{\upsilon} \tag{3}$$

2. Experimental procedure

2.1. Materials

The experiments used twice distilled CCl_4 (Aldrich 99.9% HPLC grade), twice distilled DCE (Mallinckrodt, AR), and twice distilled DCM (Aldrich, 99.9% A.C.S. HPLC). The $CHCl_3$ used was also purchased from Aldrich (>99.9% Chromosolv Plus for HPLC with 0.5% ethanol stabilizer) and was extracted twice with water to remove the ethanol. Water for the aqueous phase came from a Barnstead Nanopure II system (18 MΩ cm). The sample cell and all glassware used in the experiments were soaked in concentrated sulfuric acid containing NoChromix and then rinsed thoroughly with 18 MΩ water.

2.2. Methods

Two laser systems were used to carry out the VSFS experiments presented here. Details of the first laser system have been described previously [24]. Briefly, the system consists of a Nd:YAG laser (Coherent Infinity-100) with 1064 nm output, 3.5 ns pulse width, and a 20 Hz repetition rate. The beam is split with one portion being frequency doubled to make light at 532 nm that is sent to the interface for use in experiments. The remainder of the beam is sent to an optical parametric oscillator/

optical parametric amplifier (LaserVision) that generates the tunable IR (2700–4000 cm^{-1}) using KTP and KTA crystals. For experiments utilizing this laser system, the pulse energies used are 2 mJ and ~1.2 mJ for the 532 nm visible and IR light respectively. The second laser system also uses a 532 nm visible beam generated by frequency doubling the fundamental output (28 ps pulse width, 10 Hz) from a Nd:YAG laser (EKSPLA). The IR beam is generated from an optical parametric generation/amplification and difference frequency generation system (EKSPLA) based on BBO and $AgGaS_2$ crystals that is tunable from 1000 to 4300 cm^{-1}. Pulse energies of 80 μJ of 532 nm visible light and ~150 μJ IR light were used in experiments with this laser system.

The sample set-ups were very similar for both laser systems. The visible and IR beams were overlapped at the interface in a total internal reflection (TIR) geometry, which is used to maximize the VSFS signal [35]. A photomultiplier tube collected the generated signal. A small portion of the IR beam that is split off and collected concurrent with a VSFS scan is used to normalize all spectra presented here, accounting for fluctuations in IR energies throughout the wavelength region studied. Since two different laser systems were used to acquire data for these experiments, the spectra were scaled to give comparable intensity values.

3. Results and discussion

3.1. CCl_4/water interface

The CCl_4/water interface provides a good starting point for these studies because CCl_4 is non-polar and has been well characterized already using VSFS [23,24]. Before discussing the effects of changing the polarity of the organic phase on the interfacial water structure, a brief review of the known spectral features of this interface is warranted. The spectrum of the CCl_4/water interface (Fig. 1) represents the vibrational modes of interfacial water molecules. The frequency range of 2800 – 3800 cm^{-1} that is probed in all the spectra shown below is the spectral region corresponding to OH stretch vibrations that have different degrees of interaction with neighboring water and organic molecules. By assigning peaks or regions of the spectrum to water molecules with different degrees of bonding to adjacent molecules, a structural picture is formed of water at the CCl_4/water interface.

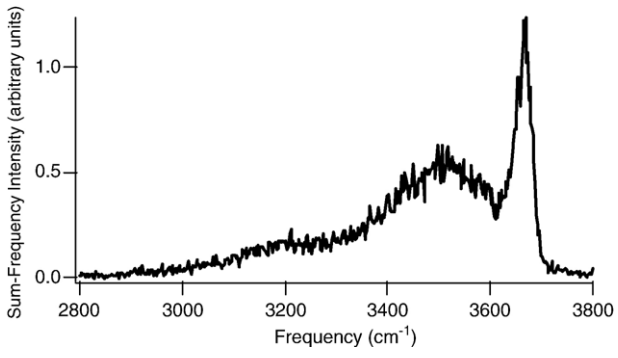

Fig. 1. Vibrational sum-frequency spectrum of the CCl_4/water interface in SSP polarization.

In VSFS, as in linear infrared spectroscopy, the lower frequency vibrational OH stretch modes of water are indicative of a more highly bonded environment. At the high frequency side of the spectrum in Fig. 1 is the sharp peak at ~3670 cm^{-1}. This is attributed to an OH stretch mode that weakly bonds to CCl_4 molecules in the interfacial region by virtue of its orientation towards the organic phase. It is referred to as the "free OH" mode. This mode is energetically uncoupled from its adjoining OH bond. This companion OH bond of such "straddling" water molecules is oriented into the aqueous phase where it can hydrogen bond to other water molecules, thus lowering its vibrational energy relative to the free OH bond. This has been designated in previous work as the "donor OH" mode because those bonds act as proton donors to surrounding water molecules. Previous isotopic dilution experiments of H_2O/D_2O mixtures have shown that this companion donor mode is near 3450 cm^{-1} [24].

The majority of VSFS spectral intensity in Fig. 1 comes from these two peaks corresponding to OH oscillators of water molecules that straddle the interface [23,24]. The strong contribution to the spectrum from these two modes is largely due to the oriented nature of these oscillators, which respond strongly in the chosen beam polarizations (SSP) that sample modes with dipole contributions perpendicular to the interfacial plane. A smaller, broader contribution at ~3200 cm^{-1} is attributed to those water molecules in the interfacial region that have more coordinated hydrogen bonding geometries. For simplicity this portion of the spectrum will be referred to as the tetrahedrally coordinated water region.

3.2. Mixture studies

Fig. 2 shows the VSFS spectra for mixtures of $CHCl_3$, DCM, and DCE with CCl_4, all at comparable mole fractions (mf) of the added polar halocarbon. From this figure a red shift of the free OH mode is evident for the three sets of spectra as the concentrations of the more polar liquids increase. Recall from Section 3.1 that the free OH peak frequency for the CCl_4/water interface is 3670 cm^{-1}. Fig. 2a shows that at the highest concentration, 0.40 mf, of added $CHCl_3$ the mode has a peak position of ~3650 cm^{-1}. At this same concentration of DCM shown in Fig. 2b, the free OH mode now has a frequency of ~3642 cm^{-1}, and for 0.40 mf DCE (Fig. 2c) it is ~3636 cm^{-1}. At concentrations of the more polar halocarbons above 0.40 mf (not shown), the free OH positions of the $CHCl_3$ and DCM mixtures do not differ significantly from the values given above. The very low signal intensity of the free OH response for the DCE mixture prohibits the determination of any subsequent frequency shift beyond 0.40 mf.

Clearly as the polarity of the organic phase increases the frequency of free OH shifts to lower and lower energies. These spectral shifts occurring with the addition of the more polar halocarbon molecules indicate an increased interaction between water and the adjacent halocarbon molecules. The extent of these frequency shifts to lower energy correlates with the dipole

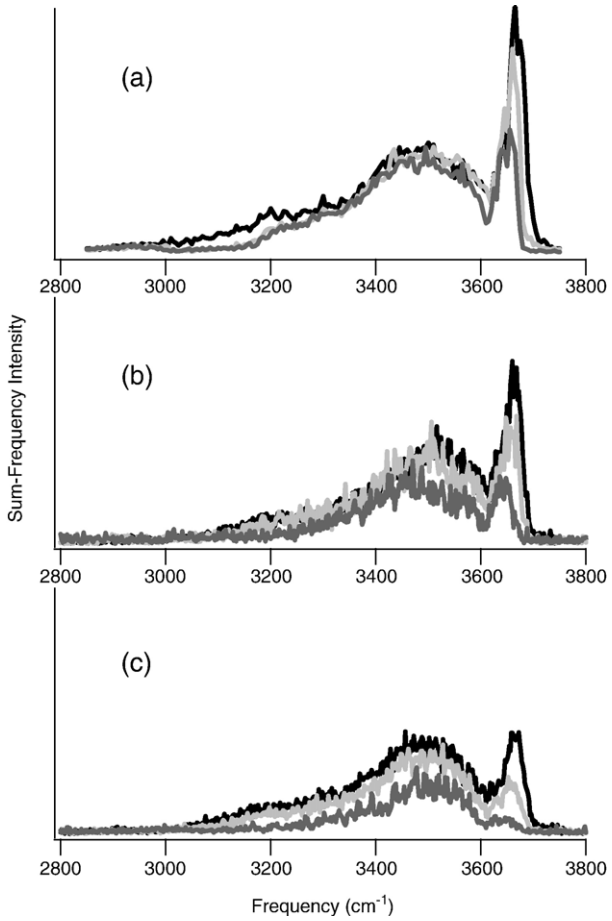

Fig. 2. Vibrational sum-frequency spectra of the ($CHCl_3$+CCl_4)/water (a) (DCM+CCl_4)/water (b) and (DCE+CCl_4)/water interfaces (c) at 0.06 (black), 0.12 (light gray), and 0.40 (gray) mole fraction of added polar halocarbons.

moments of the added halocarbon. $CHCl_3$ has the smallest dipole moment and its mixtures show the smallest frequency shift of the free OH mode. DCM has a larger dipole moment than $CHCl_3$ and shows a larger red shift for the same mode at the same concentration. Finally DCE, which has the largest dipole moment of the three halocarbons, shows the largest shift of the free OH peak to lower energy. The fact that spectral features, particularly the free OH peak, are clearly apparent in the initial additions of $CHCl_3$, DCM and DCE demonstrates that the initial addition does not significantly disturb the interfacial region, such as to cause a significant loss in interfacial water bonding and orientation.

Because the free OH mode originates from those water molecules that have direct contact with the non-aqueous phase, its frequency can be used as a measure of the extent of interaction that takes place at the interface. To compare the frequencies of the halocarbon–water interfaces with those of other liquid interfaces, Table 1 shows the free OH frequencies from VSFS results of three aqueous interfaces previously studied by the Richmond group as well as those taken from the spectra in Fig. 2 [22,24,36]. For these systems, the frequencies of the free OH from liquid–liquid interfaces are red shifted compared to that of the air/water interface. Comparing the CCl_4 and alkane interfaces, their respective free OH frequencies show that water molecules at the interface with CCl_4 interact to a greater degree than with the alkanes. The free OH peaks of the halocarbon mixtures in the present study exhibit the largest frequency shifts compared to the air/water interface. It should be noted that the frequencies of the halocarbon mixture peaks shown in Table 1 are not values determined by spectral fits of the data. Interferences that occur between the free OH and companion donor OH modes can alter the apparent peak frequency somewhat and should be taken into consideration. Work on fitting this data, which will be part of a future publication, shows that indeed the observed peak shift of the free OH to lower energy is real and not merely an interference effect. Everything to date shows that for these interfaces the water molecules at the outermost layer of the interface are participating in increased dipole–dipole type interactions with the more polar halocarbon molecules added to the non-aqueous phase.

These conclusions are supported by very recent molecular dynamics (MD) simulations done in our laboratory that calculate VSFS spectra of the CCl_4/water, (CCl_4+DCE)/water, and DCE/water interfaces [37]. The results of these studies show that there are stronger interactions between water and DCE molecules than are present between water and CCl_4. These increased interactions result in a red shift of the free OH of the computational spectra when more DCE is present in the mixed organic phase just as is described above. In addition to these MD results, several other simulations from different groups also corroborate the picture formed by the present VSFS studies. Benjamin's simulations show that stronger DCE-water interactions versus CCl_4-water are responsible for longer lifetimes of hydrogen bonds at the respective interfaces [11]. MD simulations by Dang show that the binding energy for the DCM-water dimer is stronger than that of the CCl_4-water interaction [13].

With the addition of the different polar liquids, there is also an accompanying decrease in spectral intensity for all three sets of mixtures presented. As shown in Fig. 2, the free OH, the donor OH, and the tetrahedral region in all three sets of spectra show loss of intensity as the concentrations of $CHCl_3$, DCM, and DCE increase. Like the dipole dependent trend seen in the frequency shift of the free OH, there is also a qualitative correlation between the amount of VSFS signal intensity loss

Table 1
Free OH peak frequencies from both previous VSFS studies and the present halocarbon mixture–water interfaces

Non-Polar Phase	Free OH Frequency (cm^{-1})
Air	3706 [a, b]
Alkanes	3674 [a, c]
CCl_4	3669 [a, d]
$CHCl_3$+CCl_4	3650
DCM+CCl_4	3642
DCE+CCl_4	3636

The mixtures here are all 0.40 mf of the added halocarbon and 0.60 mf CCl_4.
[a] Values are from non-linear least squares fit to the data points.
[b] Ref. [36].
[c] Ref. [22].
[d] Ref. [24].

seen in the spectra of the mixtures and the polarity of the added liquid, i.e. when comparing spectra of similar mixture concentrations the greater the dipole moment of the added liquid, the greater the loss of intensity. The spectra shown in Fig. 2a of mixtures of CCl_4 with the least polar halocarbon, $CHCl_3$, show the least loss in spectral intensity. At the highest concentration of $CHCl_3$, the three peaks in the spectrum can still be clearly distinguished. In contrast, Fig. 2c shows that at a similar concentration of DCE, the liquid that has the highest dipole moment, there is very little intensity in the tetrahedrally bonded and free OH spectral regions and a large decrease at intermediate frequencies. DCM has a polarity that is between those of $CHCl_3$ and DCE. The spectrum in Fig. 2b with the highest concentration of DCM shows loss of signal intensity that is greater than that of the $CHCl_3$ mixture but less than that of the DCE mixture for the same concentration. There are still contributions from the free OH and companion donor OH modes but no significant intensity in the tetrahedral region for the DCM and CCl_4 mixture. The spectra for concentrations of the more polar halocarbon mixtures above 0.40 mf (not shown) reveal that the VSFS intensity continues to decrease for all three mixtures but does not disappear completely. The VSFS spectrum of the neat DCE/water interface has been shown to have very weak signal that is broad and largely featureless [25].

As stated in Section 1.2, the combination of beam polarizations used in these VSFS experiments probes those vibrational modes that are perpendicular to the interface thus giving an indication of the orientation of the molecules at the interface. VSFS signal is dependent not only on the number of oscillators at the interface (see Eq. (2)) but also on how they are oriented. We conclude that the loss in spectral features that accompany the overall loss in intensity is also a result of the increased interfacial halocarbon–water interactions that occur with increased halocarbon polarity. This increased interaction leads to a decrease in oriented OH oscillators, particularly the free OH and donor OH modes that dominate the CCl_4/water spectrum. Such a loss in oriented water molecules indicates that this stronger water–halocarbon interaction leads to more randomly oriented interfacial water molecules, and likely a more diverse set of bonding interactions. Another result of the greater interaction between the more polar halocarbon molecules and a wider array of water–water interactions is a reduction in the number of interfacial water molecules that have energetically uncoupled OH oscillators (i.e. those that have a free and donor OH mode). Consequently the number of uncoupled and oriented water molecules that straddled the interface and were responsible for the large portion of spectral intensity for the water–non-polar organic interface are reduced as the interfacial water molecules adopt a broader distribution of angles and bonding interactions with the adjacent molecules. The trends observed in the intensity and spectral shifts for the three added halocarbons of increasing polarity are consistent with these conclusions.

The previously mentioned MD simulations conducted on the DCE/water interface have shown that local field corrections are also responsible for some VSFS intensity decrease compared to the CCl_4/water spectrum [37]. Due to the unknown indices of refraction of the mixed halocarbon organic phases that were studied, these corrections were not made to the spectra in Fig. 2 and could account for some of the intensity loss shown. However these simulation results have also shown that there are an increased number of oriented but very weakly hydrogen bonded and non-bonded water molecules present in the organic-rich phase at the DCE/water interface compared to the CCl_4/water interface. These oriented and weakly bonded species contribute to the VSFS spectrum to reduce the intensity of the free OH and donor OH peaks through destructive interference, resulting in an overall loss in VSFS intensity for the DCE/water interface. The penetration of more water molecules into the organic-rich phase at the DCE/water interface supports the picture formed above of increased interaction of the aqueous phase with the more polar halocarbon organic phase.

Another set of very recent MD simulations done in this laboratory also supports the above arguments about the degree of orientation of water molecules at the interface with different halocarbons [38,39]. In these studies, the tilt and twist angles of interfacial water molecules are calculated for the CCl_4/water, $CHCl_3$/water, and DCM/water interfaces. Order parameters based on these angles showed the same trend that is described in this section. The water molecules were most highly ordered at the interface with CCl_4, less ordered at the interface with $CHCl_3$, and showed the least ordering at the interface with DCM. These studies also support the picture of an increasing penetration of oriented and weakly bonded water into the organic-rich phase with increased polarity of the organic phase. Because of the nature of VSFS, if the water molecules are becoming less ordered as the organic phase becomes more polar the resulting intensity should decrease as is observed in the present studies.

4. Summary

The halocarbon/water interface has been examined using VSFS in order to further elucidate a picture of the structure and bonding that occurs at the interface between two immiscible liquids as the organic phase becomes increasingly polar. Mixtures of non-polar CCl_4 with three polar solvents, $CHCl_3$, DCM, and DCE, were used to vary the polarity of the organic phase at the interface with water providing insight into how the interactions between the two phases change as the dielectric properties of the non-aqueous phase become more and more like that of water. The resulting VSFS spectra of these mixtures showed that the free OH peak of each halocarbon mixture shifted to lower frequency as increasing amounts of polar halocarbon were added to CCl_4, in comparison to its position in the neat CCl_4/water spectrum. The magnitude of the frequency shift was smallest for $CHCl_3$, larger for DCM, and largest for DCE showing a dipole moment dependence on the extent of the red shift of the free OH mode. Just as those spectral peaks from water vibrations that have lower frequencies indicate a higher degree of hydrogen bonding, the shift of the free OH mode frequency to lower energies points to greater water-organic interactions at the interface. This spectral trend suggests that the more polar an interface is, the greater the extent of dipole-like bonding that takes place between the molecules of the organic and water phases.

The spectra also showed a decrease in intensity as the more polar liquids were added. The amount of intensity lost at a given concentration for the added polar halocarbon liquids followed the same dipole dependent trend as the free OH frequency shift. The mixtures with DCE showed the greatest loss in intensity and those with $CHCl_3$ showed the least, with the DCM mixtures having an intermediary decrease. The increased polarity of the organic phase upon addition of the more polar halocarbon to CCl_4 results in a stronger interaction between water and the interfacial organic halocarbons and a reduction in the number and orientation of the uncoupled OH oscillators that are found to dominate the spectrum for water adjacent to a non-polar liquid such as CCl_4.

The structure and bonding of water near a hydrophobic surface has been a topic of discussion and debate for many decades. Much of this interest arises because of the central role that water plays in so many biological processes. In many theoretical studies, the hydrophobic surface used for modeling interfacial water behavior is assumed to be largely non-interacting, truly hydrophobic. Although these are overly simplistic models when applied to biomolecular systems with domains and chemical constituents that can interact with water with varying degrees of attraction, these theoretical studies have set the framework for current and future studies of more complex systems. Valuable to this effort are experimental insights into how water behaves as the hydrophobic surface takes on increasingly polar character. The present VSFS studies have done this by systematically varying the polarity of the non-aqueous halocarbon phase in order to observe the effect on the interfacial region and within it, the water structure. In the future, looking at the influence of ions, pH, and possibly other types of non-polar liquids such as aromatics will further the knowledge and understanding of the critical interactions that govern so many important processes.

Acknowledgements

The authors would like to thank the National Science Foundation (grant CHE 0652531) and the Office of Naval Research (N00014-07-1-0596) for supporting this work. They also gratefully acknowledge Dr. Dennis Hore and Dave Walker for providing discussions of the MD results included in the paper.

References

[1] A.G. Volkov, D.W., Deamer, Liquid–liquid interfaces: theory and methods, ed., CRC Press, Boca Raton, FL, 1996.
[2] G.M. Luo, S. Malkova, S.V. Pingali, D.G. Schultz, B.H. Lin, M. Meron, I. Benjamin, P. Vanysek, M.L. Schlossman, J. Phys. Chem., B 110 (10) (2006) 4527.
[3] G.M. Luo, S. Malkova, S.V. Pingali, D.G. Schultz, B.H. Lin, M. Meron, T.J. Graber, J. Gebhardt, P. Vanysek, M.L. Schlossman, Electrochem. Commun. 7 (6) (2005) 627.
[4] D.M. Mitrinovic, A.M. Tikhonov, M. Li, Z.Q. Huang, M.L. Schlossman, Phys. Rev. Lett. 85 (3) (2000) 582.
[5] D.M. Mitrinovic, Z.J. Zhang, S.M. Williams, Z.Q. Huang, M.L. Schlossman, J. Phys. Chem., B 103 (11) (1999) 1779.
[6] A.M. Tikhonov, D.M. Mitrinovic, M. Li, Z.Q. Huang, M.L. Schlossman, J. Phys. Chem., B 104 (27) (2000) 6336.
[7] C.L. Beildeck, W.H. Steel, R.A. Walker, Faraday Discuss. 129 (2005) 69.
[8] E.A. McArthur, K.B. Eisenthal, J. Am. Chem. Soc. 128 (4) (2006) 1068.
[9] I. Benjamin, J. Chem. Phys. 97 (2) (1992) 1432.
[10] I. Benjamin, Chem. Phys. Lett. 393 (4–6) (2004) 453.
[11] I. Benjamin, J. Phys. Chem., B 109 (28) (2005) 13711.
[12] T.M. Chang, L.X. Dang, J. Chem. Phys. 104 (17) (1996) 6772.
[13] L.X. Dang, J. Chem. Phys. 110 (20) (1999) 10113.
[14] P. Jedlovszky, J. Phys., Condens. Matter 16 (45) (2004) S5389.
[15] P. Jedlovszky, A. Vincze, G. Horvai, J. Chem. Phys. 117 (5) (2002) 2271.
[16] P. Jedlovszky, A. Vincze, G. Horvai, Phys. Chem. Chem. Phys. 6 (8) (2004) 1874.
[17] D. Michael, I. Benjamin, J. Chem. Phys. 114 (6) (2001) 2817.
[18] R.L. Napoleon, P.B. Moore, J. Phys. Chem., B 110 (8) (2006) 3666.
[19] K.J. Schweighofer, I. Benjamin, J. Electroanal. Chem. 391 (1–2) (1995) 1.
[20] S. Senapati, M.L. Berkowitz, Phys. Rev. Lett. 8717 (17) (2001).
[21] H.B. Wang, E. Carlson, D. Henderson, R.L. Rowley, Mol. Simul. 29 (12) (2003) 777.
[22] M.G. Brown, D.S. Walker, E.A. Raymond, G.L. Richmond, J. Phys. Chem., B 107 (1) (2003) 237.
[23] L.F. Scatena, M.G. Brown, G.L. Richmond, Science 292 (5518) (2001) 908.
[24] L.F. Scatena, G.L. Richmond, J. Phys. Chem., B 105 (45) (2001) 11240.
[25] D.S. Walker, M. Brown, C.L. McFearin, G.L. Richmond, J. Phys. Chem., B 108 (7) (2004) 2111.
[26] C.D. Bain, J. Chem. Soc., Faraday Trans. 91 (9) (1995) 1281.
[27] M. Buck, M. Himmelhaus, J. Vac. Sci. Technol., A, Vac. Surf. Films 19 (6) (2001) 2717.
[28] R.W. Boyd, Nonlinear Optics, 2nd ed. Academic Press, San Diego, CA, 2003.
[29] A.G. Lambert, P.B. Davies, D.J. Neivandt, Appl. Spectrosc. Rev. 40 (2) (2005) 103.
[30] J.F. McGilp, J. Phys. D: Appl. Phys. 29 (7) (1996) 1812.
[31] P.B. Miranda, Y.R. Shen, J. Phys. Chem., B 103 (17) (1999) 3292.
[32] A.J. Moad, G.J. Simpson, J. Phys. Chem., B 108 (11) (2004) 3548.
[33] Y.R. Shen, Principles of Nonlinear Optics, ed., John Wiley & Sons, New York, 1984.
[34] H.F. Wang, W. Gan, R. Lu, Y. Rao, B.H. Wu, Int. Rev. Phys. Chem. 24 (2) (2005) 191.
[35] J. Lobau, K. Wolfrum, J. Opt. Soc. Am., B, Opt. Phys. 14 (10) (1997) 2505.
[36] E.A. Raymond, T.L. Tarbuck, M.G. Brown, G.L. Richmond, J. Phys. Chem., B 107 (2) (2003) 546.
[37] D.S. Walker, F.G. Moore, G.L. Richmond, J. Phys. Chem., C 111 (16) (2007) 6103.
[38] D.K. Hore, D.S. Walker, L. MacKinnon, G.L. Richmond, J. Phys. Chem., C 111 (25) (2007) 8832.
[39] D.K. Hore, D.S. Walker, G.L. Richmond, J. Am. Chem. Soc. 129 (4) (2007) 752.